The Astrophysical Journal Letters, 771:L41 (5pp), 2013 July 10 doi:10.1088/2041-8205/771/2/L41
© 2013. The American Astronomical Society. All rights reserved. Printed in the U.S.A.

DISCOVERY OF NUCLEAR WATER MASER EMISSION IN CENTAURUS A

Jürgen Ott[1], David S. Meier[1,2], Mark McCoy[2], Alison Peck[3], Violette Impellizzeri[3,4], Andreas Brunthaler[5], Fabian Walter[1,6], Philip G. Edwards[7], Crystal N. Anderson[2], Christian Henkel[5,8], Ilana Feain[7], and Minnie Y. Mao[1]
[1] National Radio Astronomy Observatory, P.O. Box O, 1003 Lopezville Road, Socorro, NM 87801, USA; jott@nrao.edu, dmeier@nmt.edu, walter@mpia.de, mmao@nrao.edu
[2] New Mexico Institute of Mining and Technology, 801 Leroy Place, Socorro, NM 87801, USA; mmccoy@nmt.edu, canderso@nmt.edu
[3] National Radio Astronomy Observatory, 520 Edgemont Road, Charlottesville, VA 22903, USA; apeck@nrao.edu, vimpelli@alma.cl
[4] Joint ALMA Observatory, Alonso de Córdova 3107, Vitacura 763 0355, Santiago de Chile, Chile
[5] Max-Planck Institut für Radioastronomie, Auf dem Hügel 69, D-53121 Bonn, Germany; brunthal@mpifr-bonn.mpg.de, chenkel@mpifr-bonn.mpg.de
[6] Max-Planck-Institut für Astronomie, Königstuhl 17, D-69117, Heidelberg, Germany
[7] CSIRO Astronomy and Space Science, P.O. Box 76, Epping, NSW 1710, Australia; Phil.Edwards@csiro.au, Ilana.Feain@csiro.au
[8] Astronomy Department, Faculty of Science, King Abdulaziz University, P.O. Box 80203, Jeddah, Saudi Arabia
Received 2013 May 12; accepted 2013 May 28; published 2013 June 27

ABSTRACT

We report the detection of a 22 GHz water maser line in the nearest ($D \sim 3.8$ Mpc) radio galaxy Centaurus A (Cen A) using the Australia Telescope Compact Array (ATCA). The line is centered at a velocity of ∼960 km s^{-1}, which is redshifted by about 415 km s^{-1} from the systemic velocity. Such an offset, as well as the width of ∼120 km s^{-1}, could be consistent with either a nuclear maser arising from an accretion disk of the central supermassive black hole (SMBH), or with a jet maser that is emitted from the material that is shocked near the base of the jet in Cen A. The best spatial resolution of our ATCA data constrains the origin of the maser feature within <3 pc of the SMBH. The maser exhibits an isotropic luminosity of ∼1 $L_{\odot}$, which classifies it as a kilomaser, and appears to be variable on timescales of months. A kilomaser can also be emitted by shocked gas in star-forming regions. Given the small projected distance from the core, the large offset from systemic velocity, and the smoothness of the line feature, we conclude that a jet maser line emitted by shocked gas around the base of the active galactic nucleus is the most likely explanation. For this scenario we can infer a minimum density of the radio jet of $\gtrsim$10 cm^{-3}, which indicates substantial mass entrainment of surrounding gas into the propagating jet material.

Key words: galaxies: individual (Centaurus A, NGC 5128) – ISM: jets and outflows – masers

1. INTRODUCTION

Centaurus A (Cen A) is by far the nearest radio galaxy and one of the brightest radio sources in the sky. Its proximity of only 3.8 Mpc (Harris et al. 2010) makes it a unique target for studies of supermassive black hole (SMBH) accretion, jet formation and acceleration, and the interaction of the jets and lobes with the interstellar and intergalactic media.

Cen A (see Israel 1998 for a review of the properties of Cen A) is embedded in the giant elliptical host NGC 5128. Unlike most other elliptical galaxies, NGC 5128 displays very prominent dust lanes that are likely due to merger activity in the past (see, e.g., Israel 1998; Barnes 2002; Auld et al. 2012 and references therein). NGC 5128 may thus be in the process of rebuilding a strongly warped, gaseous disk (e.g., Quillen et al. 2006, 2010; Neumayer et al. 2007; Struve et al. 2010) that shows signatures of spiral arms (Espada et al. 2012). These properties may affect the gas accretion processes onto the active SMBH (mass: $\sim 5.5 \times 10^7$ $M_{\odot}$; Cappellari et al. 2009).

The 22 GHz water (H_2O) masers have proven to be great tools to study the environments close to SMBHs. Water masers are collisionally pumped (e.g., Kylafis & Norman 1991) and the requisite high gas densities are typically achieved in shock fronts. Thus, H_2O masers can be found in very diverse environments. Typical locations include shells of expanding asymptotic giant branch stars, expanding envelopes of young stellar objects, accretion disks of SMBHs, and interaction zones of radio jets with the surrounding media (see Lo 2005 for a review). The latter two are often referred to as "disk masers" (e.g., Greenhill et al. 1995; Lo 2005) and "jet masers" (e.g., Claussen et al. 1998; Peck et al. 2003). Studying nearby jet and disk masers may also lead to a better understanding of SMBHs in the high-redshift regime. Due to their brightness, 22 GHz water masers have been observed up to $z \sim 2.64$ (Impellizzeri et al. 2008; Castangia et al. 2011).

In the past, Cen A was the target of a number of unsuccessful H_2O maser emission searches (e.g., Claussen & Lo 1986; Braatz et al. 1996, 2004; Surcis et al. 2009). In the following, we report the first detection of a water maser toward the nuclear environment of Cen A. Our observations and data reduction steps are described in Section 2, followed by a presentation of our results in Section 3, and a discussion on the nature of the detected maser feature in Section 4. We summarize our findings in Section 5.

2. OBSERVATIONS AND DATA REDUCTION

We observed Cen A with the Australia Telescope Compact Array (ATCA). The ATCA is a six-antenna interferometer with baselines between 30 m and 6 km. The observations were performed around the rest frequency of the $J = 6_{16}$–5_{23} water transition at 22.23508 GHz. We used the Compact Array Broadband Backend (Wilson et al. 2011) in two different modes: a wide-band mode, with a total bandwidth of two times 2 GHz and a channel width of 1 MHz (or 13 km s^{-1} velocity resolution; CFB 1M-0.5k mode) and CFB 64M-32k mode, where we tuned one of the 64 MHz wide zooms to water (total velocity range of ∼860 km s^{-1}; channel width of 23 kHz or 0.4 km s^{-1}). To exclude cross-identification of instrumental features with the water line and to reduce systematic effects, we observed at different central frequencies (see Table 1). After cropping bandpass edges, the velocity range

Table 1
Summary of the ATCA Observations

Date	Array	$\nu_{\rm center}$ (GHz)	BW (MHz)	Beam Size ($''$)	Beam P.A. (deg)	$S_{\rm cont}$ (Jy)	rms (mJy beam^{-1})	Δv (km s^{-1})	$t_{\rm int}$ (hr)
(1)	(2)	(3)	(4)	(5)	(6)	(7)	(8)	(9)	(10)
2011 Jul 16	H 214	22.450	1000	8.32×6.59	82.3	6.6 ± 1.0	10	13	8
2011 Oct 1	H 75	22.450	1000	26.80×20.68	87.9	8.2 ± 1.2	5	13	9
2012 Mar 27	H 168	22.494	1000	12.22×8.84	82.7	8.1 ± 1.2	4	13	8
2012 Mar 29	H 168	22.172	64	12.30×9.46	77.5	7.63 ± 0.76	3	0.4	10
2012 May 22	6 D	22.172	64	0.79×0.32	18	8.66 ± 0.87	6	0.4	8
2013 Feb 21	6 A	22.162	64	1.23×0.36	-26.5	6.58 ± 0.66	15	0.4	5.5

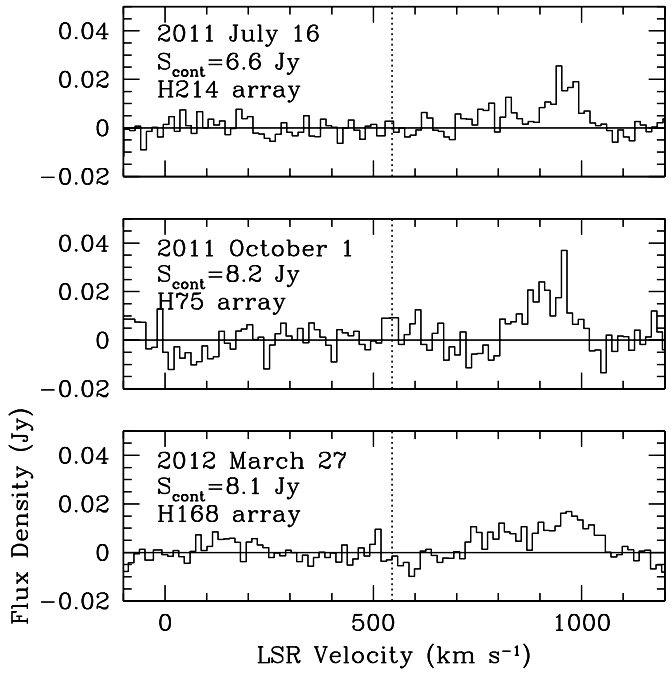

Figure 1. Spectra from three different epochs of ATCA observations in the broadband mode. The dashed vertical lines indicate the systemic velocity of NGC 5128 (545 km s^{-1} LSRK). The shown spectra cover the -100 km s^{-1} to 1200 km s^{-1} range of the full 1 GHz observations.

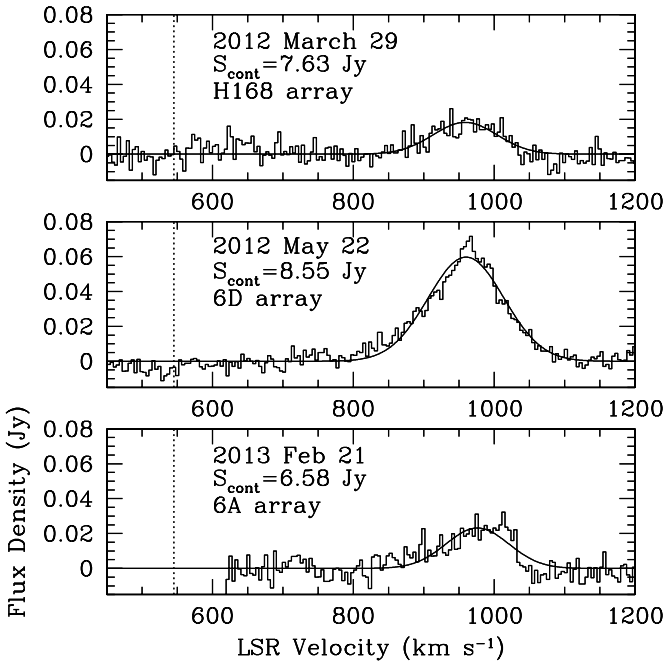

Figure 2. Narrow-band spectra of the Cen A water maser line at three different epochs. The dashed vertical lines again indicate the systemic velocity of NGC 5128 (545 km s^{-1} LSRK). The best-fitting Gaussian is shown on the top of each spectrum.

of the narrow-band observations amounts to ∼620–1380 km s^{-1} for a central frequency of 22.172 GHz and ∼440–1290 km s^{-1} for 22.272 GHz. Absolute fluxes were calibrated with the ATCA standard PKS 1934-638. Bandpasses were typically obtained by observing PKS 1253-055 for ∼15 minutes, but we used PKS 0537-441 when the former was not available at the start of the observations. The observational setups and properties are summarized in Table 1, where we list the dates of the observations in column 1, the ATCA array configurations in column 2, the central frequencies $\nu_{\rm center}$ and bandwidths BW of the instrumental setups in columns 3 and 4, the beam sizes and position angles in columns 5 and 6, the continuum flux densities $S_{\rm cont}$ in column 7, and the rms noise values, the channel separations, and the on-source integration times $t_{\rm int}$ in columns 8–10, respectively.

The data were self-calibrated on the strong continuum emission from the core of Cen A to correct phase and gain variations as a function of time. Finally, we extracted spectra from the image cubes after robust weighting and cleaning of 1000 iterations per channel. All data reduction steps were performed in MIRIAD. Whereas the narrow-band observations show sufficiently flat baselines fitted well by zeroth-order polynomials, the wide-band observations exhibit continuum flux density variations of the order of ∼1%–2%. Given the relatively high flux densities of the central source (see Table 1), these variations amount to a ∼100 mJy level, and we fitted and subtracted third-order polynomials to a ∼2000 km s^{-1} velocity range around the water frequency for satisfactory results. Given the spectral variations of the baselines, we estimate ∼10% uncertainty for the absolute fluxes of the well-behaved narrow-band observations, and a conservative ∼15% error for the wide-band data.

3. RESULTS

We extracted line emission at the central position of the SMBH at R.A. (J2000) = $13^{\rm h}25^{\rm m}27\overset{\rm s}{.}6$, decl. (J2000) = $-43^\circ01'09''$ and subtracted the continuum emission. The wide-band spectra are shown in Figure 1 and the narrow-band data in Figure 2. The systemic velocity of Cen A is at a kinematic local standard of rest (LSRK) value of ∼545 km s^{-1} (Saviane & Jerjen 2007) and we mark this value in the figures, assuming that the line can be identified as the $J = 6_{16}$–5_{23} water maser transition at a rest frequency of 22.23508 GHz (see Section 4.2). We clearly detect a spatially unresolved emission feature at

Table 2
Properties of the Gaussian Fits to the Narrow-band Spectra

Date	v_c (LSRK) (km s^{-1})	$v_{\rm FWHM}$ (km s^{-1})	$S_{\rm p}$ (mJy)	$L_\odot$
(1)	(2)	(3)	(4)	(5)
2012 Mar 29	959 ± 4	107 ± 11	18.2 ± 2.3	0.7 ± 0.1
2012 May 22	960 ± 1	127 ± 3	59.8 ± 6.1	2.7 ± 0.3
2013 Feb 21	965 ± 5	126 ± 12	23.1 ± 2.9	1.0 ± 0.1

$\sim$950 km s^{-1} offset from the systemic velocity. No detections are seen at systemic and blueshifted velocities. As the narrow-band observations resulted in higher quality spectra, we used these data to constrain the line properties. Although the lines do not appear to be perfectly Gaussian in shape, we nevertheless fitted one-component Gaussians to these lines. The results are listed in Table 2 and plotted in Figure 2. The table contains the dates of the observations in column 1, followed by the best-fit central LSRK velocities v_c, the FWHMs of the fitted line $v_{\rm FWHM}$, and the peak fluxes S_p in columns 2–4. In column 5, we list the derived isotropic luminosity values in units of $L_\odot$. The resulting parameters reveal that the H_2O maser line is at a velocity of $\sim$960 km s^{-1}, redshifted $\sim$415 km s^{-1} from systemic, with a width of $\sim$120 km s^{-1}. The amplitude is $\sim$20 mJy with the exception of the data taken on 2012 May 22, where we find a three times higher peak flux density of $\sim$60 mJy. The continuum flux at this epoch is only about 30% higher than the lowest measured continuum flux at all epochs, whereas the line is $\sim$3 times stronger. Although some continuum variations could be due to the different synthesized beam sizes of the individual observations (see Table 1), this suggests that the variation is predominantly intrinsic to Cen A.

4. DISCUSSION

4.1. Location of the Line Emission

Our observations are consistent with unresolved line emission emerging from the center of Cen A. For each of the 6 km array data, the synthesized beam sizes (see Table 1) correspond to physical resolutions of about 14.6 pc $\times$ 5.9 pc and 22.7 pc $\times$ 6.6 pc. The position angles of the two observations are separated by $\sim$40°, and we can assume that the line is emitted from within the overlap region with a conservative upper limit of a maximum of $<$3 pc projected distance away from the SMBH.

4.2. Line Identification

We observe the line feature at a sky frequency of $\sim$22.162 GHz. If the line would originate in Cen A at its systemic velocity of 545 km s^{-1} LSRK, the line rest frequency would be expected to be close to a value of $\sim$22.202 GHz. Adding a potential velocity offset of $\pm$1000 km s^{-1} (or $\pm$75 MHz), the following astrophysical spectral lines other than the H_2O $J = 6_{16}$–5_{23} maser transition with a rest frequency of 22.23508 GHz could be candidates for the emission in Cen A[9]: CH_2OHCHO $J = 4_{13}$–4_{04} at a rest frequency of 22.143 GHz, $C^{13}CS$ $J = 1_2$–0_1 at $\sim$22.255 GHz, and CCO $J = 1_2$–0_1 at 22.258 GHz. None of these lines are expected to be bright enough to explain the observed intensities. And none of them lie near the systemic velocity, requiring very unusual kinematics if they would be emitted from a molecular cloud that is located at a projected distance no farther than 3 pc from the core of Cen A (Section 4.1). In addition, given the strong continuum of Cen A, all of the thermal lines are more likely to be detectable in absorption and not emission (Cen A has a complex molecular absorption spectrum as shown in, e.g., Eckart et al. 1990; Israel 1992, 1998; Wiklind & Combes 1997; Muller & Dinh-V-Trung 2009; Espada et al. 2010). Apart from the molecules, the H 83β radio recombination line has a rest frequency of 22.196 GHz and could be a potential candidate for the emission. But given that we do not even see any Hα recombination lines in our wide-band spectra, we can exclude an identification with the much weaker Hβ line. The only likely line candidate is the redshifted H_2O $J = 6_{16}$–5_{23} maser transition, which is by far the brightest astrophysical transition across the observed frequency range. As alluded to in Section 1, H_2O has also been observed toward the nuclei of other active galaxies, and the maser line is the most likely one observed in emission in the presence of Cen A's strong continuum emission.

[9] As taken from the Lovas catalog: http://physics.nist.gov/cgi-bin/micro/table5/start.pl

4.3. Maser Strength

The maser feature has a FWHM of $\sim$120 km s^{-1}, which shows some single-channel peaks in the wide-band data (Figure 1) but is relatively smooth in the narrow-band data, where we cannot decompose the spectra into more narrow individual maser features down to our $\sim$1 km s^{-1} velocity resolution. We may thus assume that the line emerges from a single maser spot unless high-resolution imaging will break it up into more components. The isotropic luminosity of the feature is $\sim 1\,L_\odot$ (see Table 2), and it falls into the category of kilomasers. H_2O masers of similar strengths are found in nearby, moderately star-forming galaxies and mergers, such as M51, NGC 253, M82, NGC 2146, NGC 3556, NGC 3620, or the Antennae (Claussen et al. 1984; Ho et al. 1987; Nakai & Kasuga 1988; Tarchi et al. 2002; Henkel et al. 2004; Lo 2005; Henkel et al. 2005; Surcis et al. 2009; Brunthaler et al. 2009; Brogan et al. 2010). It is also similar in strength to the Galaxy's most luminous water maser, W49N (e.g., Walker et al. 1982).

In all but one epoch, the peak of the maser feature hovers around 20 mJy. The 2012 May 22 data, however, reveal a line three times stronger (see Section 3). The variability may be related to a merely $\sim$30% stronger continuum flux at the time, which may indicate that the maser itself is unsaturated. A conclusive statement, however, requires more epochs of observations, desirably at higher spatial resolution.

4.4. Star Formation, Jet, or Disk Maser?

Most kilomasers are found in star formation regions of galaxies (see references above and, e.g., Baudry & Brouillet 1996). They typically arise from outflows of massive stars and show velocity spreads of up to a few tens of km s^{-1}. For Cen A, we can pinpoint the maser to within $<$3 pc projected distance from the nucleus (Section 4.1). We consider the probability of crossing a massive star formation region along the line of sight to be low. Even if such a region is located in that direction, the velocity offset of $\sim$400 km s^{-1} from systemic and the line width of $\sim$120 km s^{-1} would be inconsistent with a typical H_2O maser in a star-forming region well outside the nuclear region.

Strong water masers are also observed toward the accretion disks of some SMBHs ("disk masers") and close to jet–ISM interaction regions near active galactic nuclei ("jet masers"). A typical example for disk masers is the archetypical NGC 4258 galaxy (e.g., Greenhill et al. 1995; Lo 2005), and a larger sample of such masers have been observed in dedicated search

campaigns (e.g., Tarchi et al. 2002; Henkel et al. 2005; Kondratko et al. 2006; Braatz & Gugliucci 2008; Castangia et al. 2008; Bennert et al. 2009; Surcis et al. 2009; König et al. 2012). Disk masers typically have three major components: one at systemic velocities, in addition to blueshifted and redshifted line features, both offset by a few hundred km s^{-1}. Some disks, however, lack one or two of these main components. At high velocity resolution (see, e.g., Braatz & Gugliucci 2008), the disk maser components show significant substructures at km s^{-1} line-width scales. They can overlap and blend to form broader components. Although we may see some indications of substructure in the wide-band data that was observed in 2011 (see Figure 1), the overall H_2O spectrum in Cen A is relatively smooth, even at the km s^{-1} scales of our high spectral resolution data (Figure 2). We thus consider a disk maser origin unlikely unless more evidence emerges.

Jet masers, have been detected in NGC 1068 (Gallimore et al. 1996), NGC 3079 (Trotter et al. 1998), Circinus (Greenhill et al. 2003), Mrk 348 (Peck et al. 2003), and possibly in NGC 1052 (Claussen et al. 1998; Kameno et al. 2005). In particular, the jet maser in Mrk 348 resembles Cen A's maser in many respects. The line in Mrk 348 is ∼130 km s^{-1} redshifted from systemic, 130 km s^{-1} wide, and relatively smooth. Very Long Baseline Array data show that the maser is ∼1 pc away from the core. Monitoring also shows some significant line variability on timescales as short as a day, which is loosely correlated with the continuum strength (Peck et al. 2003). The isotropic luminosity of the Mrk 348 maser, however, is about two orders of magnitude higher than the feature in Cen A. We also observe similarities with the possible jet maser in NGC 1052. The H_2O line in NGC 1052 is redshifted ∼400 km s^{-1} from systemic with a line width of ∼200 km s^{-1}. Its isotropic luminosity is of the same order as the maser in Mrk 348. Given the similarities of the Cen A H_2O maser emission with the above cases, we discuss the implications of the jet maser model for Cen A in the following section.

4.5. Jet Maser Properties

A useful model for a jet maser has been established by Peck et al. (2003). They propose that the jet plows into a neighboring molecular cloud and creates a shock front that propagates away from the jet direction. The tip of the shock front covers a large opening angle, and the morphology resembles that of a mushroom, with cloud material being compressed toward the front and the sides of the jet. The projected velocities of the shocked material may thus combine to the large line width that we witness. Shocks propagate according to the density contrast between the two media at the shock boundary via $\rho_i v_i^2 = \rho_o v_o^2$, where ρ_i and v_i are the density and velocity of the initial, shocking material, and ρ_o and v_o of the propagating forward shock front in the material that was hit. Tingay et al. (1998) monitored the motions of parsec-scale jet components in Cen A and derived velocities of $v_i \sim 0.1$ c. For a shock that propagates with the velocity offset of the maser feature in Cen A, $v_o \sim 400$ km s^{-1}, we can derive a density contrast ρ_i/ρ_o of $\sim 2 \times 10^{-4}$. Interstellar H_2O masers require volume densities of at least $>10^7$ cm^{-3} (Yates et al. 1997; Lo 2005) to be pumped (see Kylafis & Norman 1991 for scenarios when radiative pumping may become important). When we apply the density contrast to this number, we can infer an incoming jet density ρ_i of $>10^3$ cm^{-3}. Geometry constraints will change the numbers, but the order of magnitude estimate should remain if the shock front has a large opening angle as suggested by Peck et al. (2003). The jet velocity, however, may be underestimated. Tingay et al. (1998) show that the northern jet is much brighter than the southern counterpart, which can be explained by Doppler boosting the brightness of the approaching jet. Such an effect would be expected at much higher velocities than the ∼0.1 c measured for the individual components. For the limit of a jet velocity at light speed, the above calculations will reduce the lower limit of the jet density by two orders of magnitude and we thus estimate a more conservative $\rho_i > 10$ cm^{-3}. But even such a reduced value is much larger than typical electron–positron or thermal gas plasma densities expected for relativistic jets. The radio galaxy 3C120, for example, has densities $\lesssim 10^{-3}$ cm^{-3} (Walker et al. 1987), which is four orders of magnitude lower than our limit for the jet of Cen A. The difference can potentially be explained by surrounding material that is evaporated by and entrained into the jet during its outward propagation.

Kameno et al. (2005) find indications for the appearance of narrow components in the otherwise broad maser spectrum of NGC 1052. These components show flux variabilities and line narrowing on timescales of days. Our 2011 ATCA broadband H_2O spectra of Cen A may show indications for similar, single-channel narrow features. In the jet maser model, such variations could be due to the jet shocking small, high-density substructures of the molecular cloud. The maser properties could be the response to the shock dynamics that includes local density enhancements, non-linear maser amplification, and possible H_2O shock dissociation.

The Cen A maser line is redshifted to velocities larger than systemic. The receding, fainter jet may thus be a natural location for the origin of the jet maser feature. We note, however, that the Very Long Baseline Array data show that the similarly redshifted H_2O maser in Mrk 348 originates from the approaching, brighter jet component of this galaxy. The full location and geometry of the maser spots in Cen A are therefore uncertain until higher resolution imaging is available.

5. SUMMARY

We report the detection of a 22 GHz $J = 6_{16}$–5_{23} water maser emission line toward the inner 3 pc of the nearest radio galaxy Cen A. The weak and slightly variable maser feature can be classified as a kilomaser and could have its origin in a star formation region, a nuclear disk around the central SMBH, or from material that is shocked close to the jet base of Cen A. Given the relative smoothness and width of the line, as well as its central location, we conclude that the "jet maser" scenario is the most likely one. In this case, the radio jet is shocking a central molecular cloud. From the shock properties, a lower limit to the density of the jet of >10 cm^{-3} can be derived. A full characterization of the nature and properties of the maser will require observations with higher spatial resolution. The discovery of a nuclear water maser in Cen A opens up further opportunities to probe the extreme environments very close to an SMBH.

We thank the Australia Telescope National Facility staff for their assistance, and gratefully acknowledge the allocation of Director's time to confirm this feature. The Australia Telescope Compact Array is part of the Australia Telescope National Facility which is funded by the Commonwealth of Australia for operation as a National Facility managed by CSIRO. The National Radio Astronomy Observatory is a facility of the National Science Foundation operated under cooperative agreement by Associated Universities, Inc. D.S.M. and M.M. acknowledge

support from NSF AST-1109803. A.B. was supported by a Marie Curie Outgoing International Fellowship (FP7) of the European Union (project number 275596). This research has made use of NASA's Astrophysics Data System and the NASA/IPAC Extragalactic Database (NED) which is operated by the Jet Propulsion Laboratory, California Institute of Technology, under contract with the National Aeronautics and Space Administration.

Facility: ATCA

REFERENCES

Auld, R., Smith, M. W. L., Bendo, G., et al. 2012, MNRAS, 420, 1882
Barnes, J. E. 2002, MNRAS, 333, 481
Baudry, A., & Brouillet, N. 1996, A&A, 316, 188
Bennert, N., Barvainis, R., Henkel, C., & Antonucci, R. 2009, ApJ, 695, 276
Braatz, J. A., & Gugliucci, N. E. 2008, ApJ, 678, 96
Braatz, J. A., Henkel, C., Greenhill, L. J., Moran, J. M., & Wilson, A. S. 2004, ApJL, 617, L29
Braatz, J. A., Wilson, A. S., & Henkel, C. 1996, ApJS, 106, 51
Brogan, C., Johnson, K., & Darling, J. 2010, ApJL, 716, L51
Brunthaler, A., Castangia, P., Tarchi, A., et al. 2009, A&A, 497, 103
Cappellari, M., Neumayer, N., Reunanen, J., et al. 2009, MNRAS, 394, 660
Castangia, P., Impellizzeri, C. M. V., McKean, J. P., et al. 2011, A&A, 529, A150
Castangia, P., Tarchi, A., Henkel, C., & Menten, K. M. 2008, A&A, 479, 111
Claussen, M. J., Diamond, P. J., Braatz, J. A., Wilson, A. S., & Henkel, C. 1998, ApJL, 500, L129
Claussen, M. J., Heiligman, G. M., & Lo, K. Y. 1984, Natur, 310, 298
Claussen, M. J., & Lo, K.-Y. 1986, ApJ, 308, 592
Eckart, A., Cameron, M., Genzel, R., et al. 1990, ApJ, 365, 522
Espada, D., Matsushita, S., Peck, A. B., et al. 2012, ApJL, 756, L10
Espada, D., Peck, A. B., Matsushita, S., et al. 2010, ApJ, 720, 666
Gallimore, J. F., Baum, S. A., O'Dea, C. P., Brinks, E., & Pedlar, A. 1996, ApJ, 462, 740
Greenhill, L. J., Booth, R. S., Ellingsen, S. P., et al. 2003, ApJ, 590, 162
Greenhill, L. J., Jiang, D. R., Moran, J. M., et al. 1995, ApJ, 440, 619
Harris, G. L. H., Rejkuba, M., & Harris, W. E. 2010, PASA, 27, 457
Henkel, C., Peck, A. B., Tarchi, A., et al. 2005, A&A, 436, 75
Henkel, C., Tarchi, A., Menten, K. M., & Peck, A. B. 2004, A&A, 414, 117
Ho, P. T. P., Martin, R. N., Henkel, C., & Turner, J. L. 1987, ApJ, 320, 663
Impellizzeri, C. M. V., McKean, J. P., Castangia, P., et al. 2008, Natur, 456, 927
Israel, F. P. 1992, A&A, 265, 487
Israel, F. P. 1998, A&ARv, 8, 237
Kameno, S., Nakai, N., Sawada-Satoh, S., Sato, N., & Haba, A. 2005, ApJ, 620, 145
Kondratko, P. T., Greenhill, L. J., Moran, J. M., et al. 2006, ApJ, 638, 100
König, S., Eckart, A., Henkel, C., & García-Marín, M. 2012, MNRAS, 420, 2263
Kylafis, N. D., & Norman, C. A. 1991, ApJ, 373, 525
Lo, K. Y. 2005, ARA&A, 43, 625
Muller, S., & Dinh-V-Trung, 2009, ApJ, 696, 176
Nakai, N., & Kasuga, T. 1988, PASJ, 40, 139
Neumayer, N., Cappellari, M., Reunanen, J., et al. 2007, ApJ, 671, 1329
Peck, A. B., Henkel, C., Ulvestad, J. S., et al. 2003, ApJ, 590, 149
Quillen, A. C., Brookes, M. H., Keene, J., et al. 2006, ApJ, 645, 1092
Quillen, A. C., Neumayer, N., Oosterloo, T., & Espada, D. 2010, PASA, 27, 396
Saviane, I., & Jerjen, H. 2007, AJ, 133, 1756
Struve, C., Oosterloo, T. A., Morganti, R., & Saripalli, L. 2010, A&A, 515, A67
Surcis, G., Tarchi, A., Henkel, C., et al. 2009, A&A, 502, 529
Tarchi, A., Henkel, C., Peck, A. B., & Menten, K. M. 2002, A&A, 389, L39
Tingay, S. J., Jauncey, D. L., Reynolds, J. E., et al. 1998, AJ, 115, 960
Trotter, A. S., Greenhill, L. J., Moran, J. M., et al. 1998, ApJ, 495, 740
Walker, R. C., Benson, J. M., & Unwin, S. C. 1987, ApJ, 316, 546
Walker, R. C., Matsakis, D. N., & Garcia-Barreto, J. A. 1982, ApJ, 255, 128
Wiklind, T., & Combes, F. 1997, A&A, 324, 51
Wilson, W. E., Ferris, R. H., Axtens, P., et al. 2011, MNRAS, 416, 832
Yates, J. A., Humphreys, E. M. L., & Richards, A. M. S. 1997, Ap&SS, 251, 285